Science of the Total Environment 994 (2025) 179990

Contents lists available at ScienceDirect

Science of the Total Environment

journal homepage: www.elsevier.com/locate/scitotenv

High ciguatoxin-producing *Gambierdiscus* clade (Gonyaulacales, Dinophyceae) as a source of toxins causing ciguatera poisoning

Shauna A. Murray [a,*], Arjun Verma [a], Mona Hoppenrath [b], D. Tim Harwood [c], J. Sam Murray [c], Kirsty F. Smith [c], Richard Lewis [d], Sarah C. Finch [e], Shikder Saiful Islam [f,1], Amna Ashfaq [a], Caroline Dornelles De Azevedo [a], Christopher J.S. Bolch [f]

[a] University of Technology Sydney, School of Life Sciences, PO Box 123 Broadway, Sydney, NSW 2007, Australia
[b] Senckenberg am Meer, German Centre for Marine Biodiversity Research (DZMB), Südstrand 44, D-26382 Wilhelmshaven, Germany
[c] Cawthron Institute, 98 Halifax Street East, Nelson 7010, New Zealand
[d] Institute for Molecular Bioscience, The University of Queensland, Brisbane, QLD, Australia
[e] AgResearch Ltd, Ruakura Research Centre, Private Bag 3123, Hamilton 3240, New Zealand
[f] Institute for Marine and Antarctic Studies (IMAS), University of Tasmania, Private Bag 129, Hobart 7001, Tasmania, Australia

HIGHLIGHTS

- *Gambierdiscus holmesii* produced M-seco-CTX4A/B - the second taxon after *G. polynesiensis* with chemically detectable P-CTXs.
- *G. bagnisii* sp. nov. *G. holmesii,* and *G. polynesiensis* are very closely related.
- *G. polynesiensis*, *G. bagnisii* sp. nov. and *G. holmesii,* were distributed throughout the Great Barrier Reef and South Pacific.
- CTXs produced by *Gambierdiscus* from Clade III may be responsible for the majority of CP in the South Pacific.

GRAPHICAL ABSTRACT

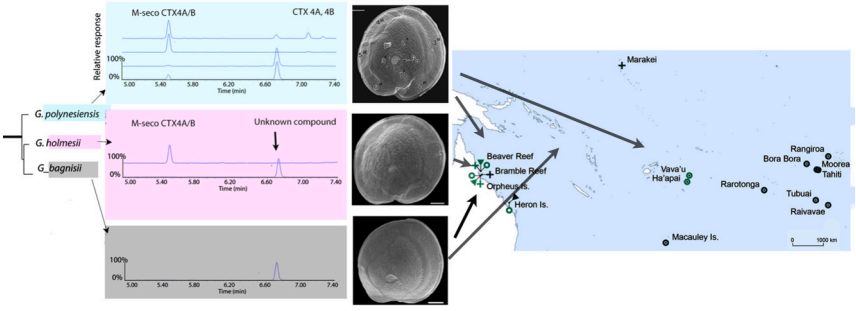

ARTICLE INFO

Editor: Elena Paoletti

Keywords:
Ciguatera poisoning (CP)
Dinophyceae
Liquid chromatography-tandem mass spectrometry (LC-MS/MS)
Morphology
Phylogeny
Ribosomal RNA

ABSTRACT

Ciguatera Poisoning (CP) is caused by neurotoxins (Ciguatoxins, CTXs) produced by microbial eukaryotes (*Gambierdiscus*, *Fukuyoa*: Dinophyceae) that accumulate in seafood and can result in severe human illness. More than 80 % of the world's CP occurs in the South Pacific, and climate change is projected to increase cases. However, our understanding of CP is hindered because *Gambierdiscus* spp. directly associated with CP remain uncertain. Most *Gambierdiscus/Fukuyoa* spp. demonstrate little CTX-like activity, which appears to be unlikely to cause CP at scale. We characterised *Gambierdiscus* from the Great Barrier Reef (Australia), a region with endemic CP, including *G. bagnisii* sp. nov., using light and scanning electron microscopy, morphometric analysis, and phylogenomics. Using LC-MS/MS, *G. holmesii* produced M-seco-CTX4A/B, the second taxon after *G. polynesiensis* with chemically detectable CTXs in the Pacific region. *G. bagnisii* sp. nov. and *G. holmesii* produced an uncharacterised compound found previously only in *G. polynesiensis*, however its bioactivity and relationship, if any, to CP is unknown. A close relationship between *G. bagnisii* sp. nov., *G. holmesii,* and *G. polynesiensis* (as Clade III)

* Corresponding author.
E-mail address: Shauna.Murray@uts.edu.au (S.A. Murray).
[1] Present address: Fisheries and Marine Resource Technology Discipline, Khulna University, Khulna, Bangladesh.

https://doi.org/10.1016/j.scitotenv.2025.179990
Received 19 February 2025; Received in revised form 13 June 2025; Accepted 24 June 2025

was found, and taxa were distributed from the far north to southern Great Barrier Reef and throughout the South Pacific. Our analyses indicate that CTXs produced by *Gambierdiscus* from Clade III, such as *G. polynesiensis*, are important in relation to CP and might be responsible for the majority of CP in the South Pacific.

Abbreviations

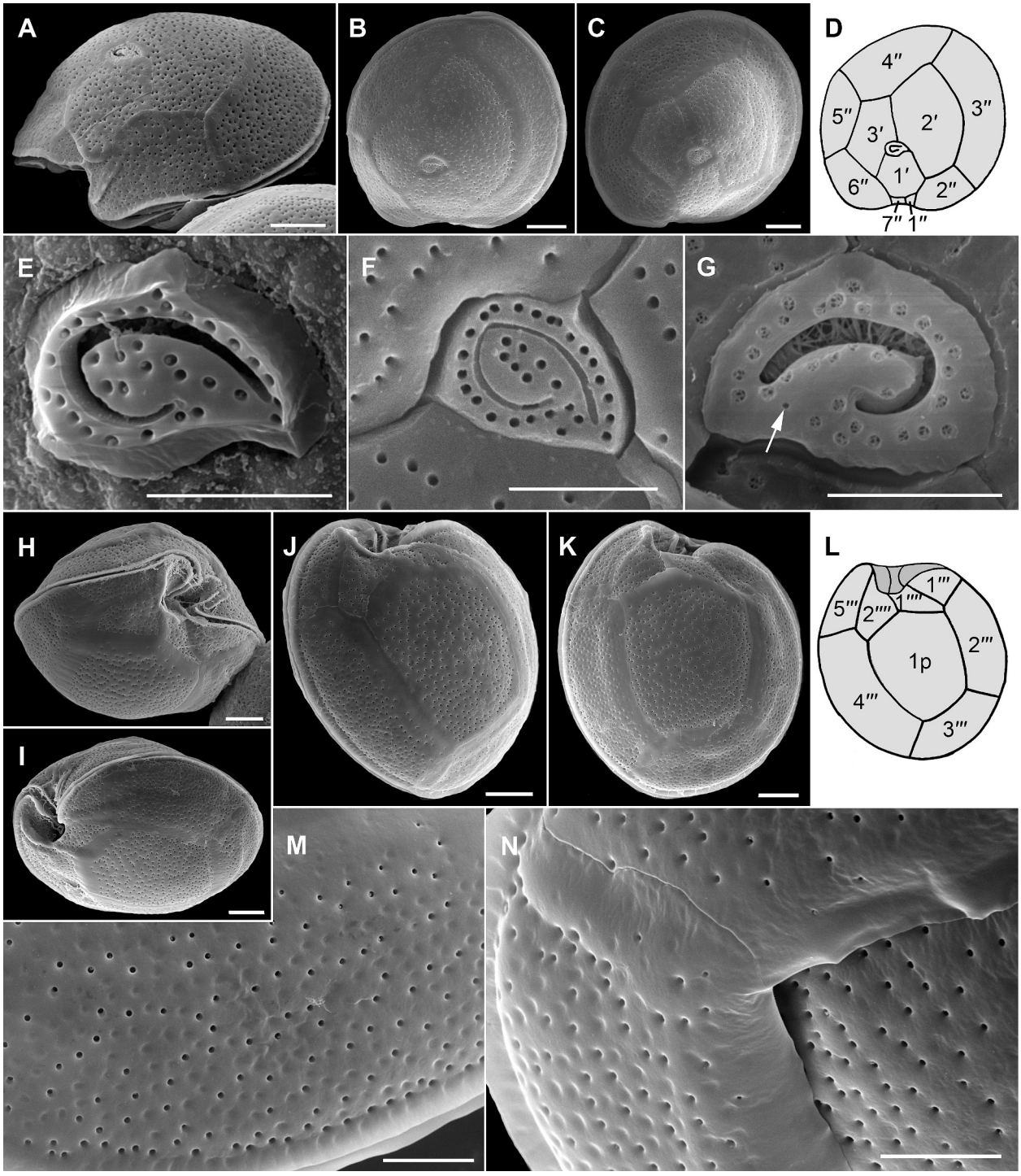

Fig. 3. A-N. Morphological analyses of *G. bagnisii* sp. nov. strain OIRS336 based on SEM. A. Epitheca, ventral to left lateral view. **B, C.** Epitheca, apical view. **D.** Line drawing of the epitheca with thecal plate designation. **E.** Isolated outer/apical pore (P_o) plate of the apical pore complex (APC). **F.** Outside view of the P_o plate. **G.** Inside view of the P_o plate. **H.** Ventral to right lateral view showing the sulcal area and cingulum displacement. **I.** Ventral to left lateral view showing the deeply excavated sulcus. **J, K.** Hypotheca, antapical view. **L.** Line drawing of the hypoheca with thecal plate designation. **M, N.** Thecal plate ornamentation showing the distribution of pores and intercalary band morphology. Note the two size classes of pores in **N**. Scale bars = 10 μm, except E-G, M, N = 5 μm.

CP ciguatera poisoning
CTX ciguatoxin
FLIPR Fluorescent Imaging Plate Reader
ITS internal transcribed spacer
LSU rDNA large sub-unit rDNA
LC-MS/MS Liquid Chromatography-Tandem Mass Spectrometry
SSU rDNA small subunit rDNA

1. Introduction

Ciguatera Poisoning (CP) is a human illness, found worldwide in tropical and sub-tropical regions, caused by the consumption of marine seafood contaminated with ciguatoxins (CTXs (Hirama et al., 2001; Inoue et al., 2004)). CTXs are produced by microbial eukaryotes (*Gambierdiscus*, *Fukuyoa*: Dinophyceae) that live epiphytically on macroalgae, seagrass, coral rubble and sometimes planktonically. More than 80 % of the world's ~ 50,000 annual CP cases occur in territories of the vast (~98,000,000 km^2) greater South Pacific Ocean, significantly affecting Pacific Small Island Developing states (Supplementary Table 1), and also Australia. The prevalence of CP can be locally high, and only a small proportion (~2–10 % of cases) are thought to be formally reported (Lehane and Lewis, 2000; Friedman et al., 2017). CTXs can be highly toxic; for example, Pacific CTX-1B has an LD_{50} of 0.25 μg kg^{-1} in mice by intraperitoneal injection (Lewis et al., 1991). Severe cases of CP in humans can result in disablement and sometimes death (Friedman et al., 2017). At least 20 of the 23 described *Gambierdiscus* and *Fukuyoa* taxa show CTX-like activity in functional bio-assays, but usually at fractions of fg $cell^{-1}$ (Hoppenrath et al., 2023) that are well below detection thresholds of chemical detection methods such as liquid chromatography-mass spectrometry (LC-MS). *Gambierdiscus* spp. producing CTX metabolites that bioconvert in the presence of fish liver S9 fractions (Ikehara et al., 2017) to CTX-1B (these metabolites are CTX4A/4B) are key to understanding and monitoring CP in the Pacific region, as P-CTX-1B is a very common, highly toxic analogue in seafood in the region. *G. polynesiensis* is the only species to date with chemically confirmed production of CTXs, including CTX4A/B, and at very high concentrations of 0.44–18.2 pg $cell^{-1}$. (Chinain et al., 2010; Rhodes et al., 2014; Longo et al., 2019a; Munday et al., 2017). Despite thousands of annual documented cases of CP in at least 18 South Pacific countries/territories (Supplementary Table 1), *G. polynesiensis* has only been found in three inhabited countries: French Polynesia, the Cook Islands, and the Kingdom of Tonga (Chinain et al., 2010; Rhodes et al., 2014; Argyle et al., 2023). It has not been detected from the majority of Pacific CP endemic locations, including Australia (Fig. 1B, C). Hence, the causative organisms associated with CP remain unknown across much of this region (Smith et al., 2023).

The Australian record of CP extends back decades (Tonge et al., 1967; Gillespie et al., 1986) (Fig. 1B, C) and includes recent southward expansion of its potential geographical range, likely related to the strengthening southwards flow of the East Australian Current (Farrell et al., 2016) (Fig. 1A). Most cases of CP in Australia are caused by fish caught in tropical waters of northern and eastern Australia, mostly in the Great Barrier Reef (GBR, (Gillespie et al., 1986; Lewis and Endean, 1984; Kohli et al., 2017)), with fewer cases in regions further south (Fig. 1B, C). Little is known of the causative species in Australian waters. Strains of *Gambierdiscus* that produced precursor metabolites of fish P-CTXs were reported from Queensland in 1991 and detected chemically using LC-MS (Holmes and Lewis, 1994; Holmes et al., 1990; Holmes et al., 1991). However, the identity of the species remains unconfirmed and no strains exist. More recent studies show that some potential CTX-producing species are present along the east coast of Australia in QLD and NSW: *G. carpenteri*, *G. honu*, *G. holmesii*, *G. lapillus*, *G. lewisii*, and *F. paulensis*, for which cultured strains showed low levels of CTX-like activity in bio-assays, but with no CTXs detected chemically (Murray et al., 2014; Kohli et al., 2014; Sparrow et al., 2017; Kretzschmar et al., 2017; Kretzschmar et al., 2019; Larsson et al., 2018).

CP increased in the southern Pacific region by 60 % over a 20-year period (Skinner et al., 2011), and climate change is projected to further increase CP (Bell et al., 2013) and expand the range and abundance of CTX-producing *Gambierdiscus*. Rising ocean temperatures, increased distributions polewards of *Gambierdiscus* spp., increased coastal nutrient loading, and increased coral bleaching and reef disturbance due to cyclones are all believed to contribute to this trend (Kohli et al., 2014; Tester et al., 2010; Rongo and Van Woesik, 2013; Chateau-Degat et al., 2005; Kibler et al., 2015; Farrell et al., 2017). Given the rapid ocean change in the South Pacific, in particular the warming East Australian Current and the GBR, and the need for improved health outcomes in Australia and Pacific Small Island Developing nations, the aim of this study was to determine the sources of CTXs in a CP endemic region by examining the identities, distribution and CTX-production in *Gambierdiscus* species.

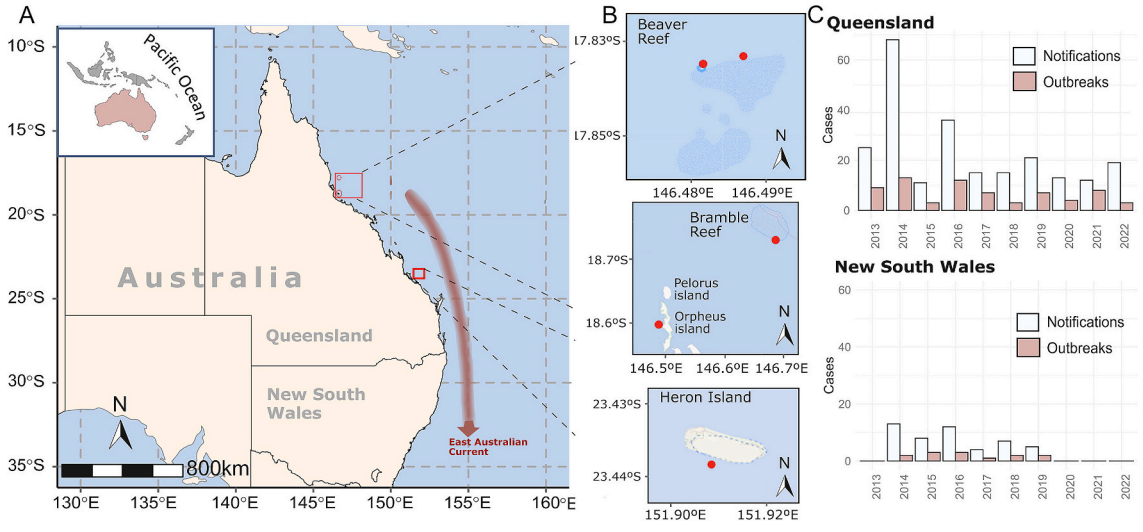

Fig. 1. **(A)** South-eastern Australia and the southwards flow of the East Australian Current. **B.** Beaver Reef, Bramble Reef, Orpheus Island and Heron Island in the GBR. **C.** Notifications of individual cases and outbreaks of CP in QLD recorded annually from 2013 to 2022 (QLD Health). **D.** Notifications of individual cases and outbreaks of CP in NSW recorded annually from 2013 to 2022 (Farrell et al., 2016).

2. Materials and methods

2.1. Field sampling, culture isolation and growth

Macroalgal thallus (*Sargassum* spp.) was collected by diving at Orpheus Island (18° 37′ S, 146° 29′ E) and at Bramble Reef (18° 27′ S, 146° 44′ E), Queensland, Australia on the 10th and 11th September 2019 (Fig. 1). Surface sea water temperatures at the sites were 25 °C and 24 °C respectively (Fig. 1A, B). Thalli were cut and placed into ziplock bags with surrounding seawater, closed and taken to the surface. Epiphytic microalgae were removed, water decanted into flasks at 24 °C for 2–4 h for dinoflagellate cells to detach, filtered through 220 μm nytal mesh onto 20 μm nytal mesh, distributed into petri dishes, and examined using a Leica MZ9.5 stereomicroscope with darkfield and brightfield illumination. *Gambierdiscus* were isolated using flame-drawn glass micropipettes. Cells were washed three times and transferred into wells of 24-well plates containing f/10 growth medium, and maintained at 25 °C (+/− 1.5 °C) at 70–100 μmol photons.m^{-2} s^{-1} light intensity (Phillips T8, cool white) with a 14:10 h light:dark cycle. After 3 weeks, surviving cultures were transferred to 12-well polystyrene plates (Costar, USA) with 3 mL of f/10 growth medium supplemented with L1 metals solution (Guillard and Hargraves, 1993). After 3 months, cultures were maintained in 70 mL tissue culture flasks (vented cap; Corning, USA) or polystyrene containers (Thermo Fisher Scientific, Australia) and subcultured every 3 weeks.

Samples for metabarcoding analyses of *Gambierdiscus* spp. were collected on Heron Island from 7th - 17th March 2018, Orpheus Island as above, and Beaver Reef on 11th October 2023. Macroalgal thalli (*Sargassum* spp., *Padina* spp.) were collected as above, shaken in local seawater, with filtrate collected on a 20 μm mesh and back-washed with sterile seawater. Samples were filtered on an 8 μm nitrocellulose filters (25 mm diameter).

2.2. Light microscopy and morphometric analyses

Thecal plates were examined using Calcofluor M2R (Fluorescent Brightener 28, Sigma) and epifluorescence microscopy (Fritz and Triemer, 1985) using a Nikon Eclipse N*i* microscope (Nikon, Japan) and Nikon DS-Ri2 camera with the software NIS-Elements BR (Nikon, Japan; v 4.40.00). Cell depth, width and height were measured under brightfield illumination ($N = 20$–40 cells per strain), and data analysed by one-way ANOVA using RStudio version 2022.07.1 + 554 with R version 4.1.0 (RCoreTeam R, n.d.). For morphometric analysis cells were imaged with the apex or antapex vertically oriented to the camera and extended depth-of-focus (EDF) images taken at 400× using NIS-elements to integrate in-focus information from multiple planes of focus (*Z*-stacks). Images were imported into FIJI (ImageJ; version 2.9.0), calibrated (1 mm; 10 μm divisions) and scaled (1 pixel = 0.073 μm; aspect ratio = 1) prior to measurement. Plate junction points were located manually and FIJI image analysis tools used to measure the linear distance (μm) between plate junctions. Analyses included only the apical (i.e., plates 1′, 2′ and 3′), antapical/Sp plate boundaries (2, 1″“, and Sp) (Fig. 2; marked red) to limit parallax and off-axis image measurement error. Distances were expressed as a ratio of cell depth, log-transformed (log (X+ 1)) and normalized prior to canonical analysis of principal coordinates (CAP) based on Euclidean distances (Primer 6.1.1.5 and PERMANOVA+ 1.0.5 (Anderson et al., 2008)) to visualize differences between *Gambierdiscus* species.

2.3. DNA extraction, PCR and sequencing of cultured strains

DNA from cultures was extracted using either a modified 3 % CTAB method (Verma et al., 2016) or a modified Urea lysis buffer method. Partial sequences of the nuclear small subunit (SSU) ribosomal RNA (rRNA), the D1 - D3 and D8 - D10 regions of the large subunit (LSU) rRNA, the internal transcribed spacer (ITS) regions, and 5.8S rRNA genes (ITS1/5.8S/ITS2) were amplified and sequenced (primers in Supplementary Table 3). PCRs were performed in 25 μL using 2× MyTaqHS, or 2× Immomix (Bioline, Australia), 0.4 μM μL^{-1} primer, 0.08 μM μL^{-1}BSA (New England Biolabs, Australia), and 1 μL DNA. Thermocycling using Immomix was 94 °C for 10 min, 35 cycles of 94 °C for 20 s, 30 s, 72 °C for 1.5 min and final extension of 72 °C for 7 min. Thermal cycling for MyTaqHS was 95 °C for 3 min, followed by 34 cycles of: 95 °C for 30 s, 20 s at 55 °C - 60.5 °C for LSU primers (53 °C for SSU primers), and extension at 72 °C for 20 s; and 10 s at 72 °C for SSU primers. PCR products were purified with DNA Clean and Concentrator (Zymo Research, Irvine, USA) or SureClean™ (Bioline, Australia) and sequenced at Macrogen Inc. (Seoul, Korea) or the Ramaciotti Centre for Genomic Analysis (Sydney, Australia).

2.4. Metabarcoding sequencing and analysis

DNA was extracted from 8 μm nitrocellulose filters using DNeasy PowerSoil Kit with modifications; samples were incubated for 1 h on ice after the addition of CD2, and spin column filter membranes were incubated for 5 min before the final elution in 80 μL and storage at −80 °C. PCR of the V4 SSU rRNA region was conducted (primers in Supplementary Table 3), and products sequenced using MiSeq v2 2x250bp at the Ramaciotti Centre for Genomic Analysis (Sydney, Australia). Trimming and processing used cutadapt (Martin, 2011), and the DADA2 pipeline (Callahan et al., 2016) respectively, with an allowed mismatch of 1.0. For the DADA2 pipeline, sequences were truncated to 350 bp and filtered for maximum “expected errors” (maxEE) of two and four for F and R reads respectively. Reads not meeting defined thresholds were discarded. Amplicon sequence variants (ASVs) were inferred based on a parametric error matrix constructed from the first 108 bp. Pair-end amplicon sequences were merged using maxmismatch = 1 and overlap = 10. Resulting ASVs were checked for chimeras, and ASVs outside the expected amplicon length were trimmed. ASVs were classified against an alignment of *Gambierdiscus* SSU rRNA sequences. ASVs with <97 % similarity to this database were removed.

2.5. Transcriptomic and phylogenetic analyses

Gambierdiscus bagnisii sp. nov. strain OIRS336 and *G. holmesii* strain OIRS406 in late exponential growth phase were centrifuged at 2500 *g* for 10 min for RNA extraction. One mL of TRI Reagent (Sigma-Aldrich, Merck, DE) was added and cells disrupted by three rounds of freeze-thaw using liquid N and 95 °C, then extracted per manufacturer's instructions. RNA eluate was purified with the RNeasy Mini Kit (Qiagen, NL) and assessed using High Sensitivity RNA ScreenTape on an Agilent 4200 Tapestation. Ramaciotti Centre for Genomics (Sydney, Australia) prepared the library using Illumina Stranded mRNA library prep kit (Illumina, USA) and sequenced using 1 lane of NovaSeq X Plus 10B 300 cycle. Sequences were quality checked and trimmed using FastQC and Trimmomatic (Bolger et al., 2014), and assembled using Trinity v2.4.0 (Haas et al., 2013), on the UTS high performance computing cluster. Homologs of 40 nuclear genes identified as core genes using BUSCO (Simao et al., 2015), were found using BLAST as implemented in Geneious Prime 2023.2.1 from sequenced transcriptomes and *G. australes* CAWD149, MMETSP0766; *G. excentricus* VGO790, SRR3348983; *G. polynesiensis* CAWD212, SRR3358210; *G. pacificus* MUR1, SRR10993127; *Ostreopsis rhodesiae* HER26, SRR9047231; *O. siamensis* BH1, SRR9038703. Alignments were determined using Clustal Omega, single gene trees were checked for polyphyly using RaxML. Final alignments were concatenated and analysed using RAxML-ng, 30 threads, a GTR + I + G model and 1000 bootstrap replicates. Bayesian phylogenetic analyses were performed using a GTR + I + G and run until the standard deviation of split frequencies was below threshold level. Chain length was 1,500,000 with a burnin of 500,000.

Sequences of the rRNA array comprised 1860 bp of SSU rRNA, 529 bp of the ITS1/5.8S/ITS2 rRNA, 972 bp of the D1-D3 region of LSU

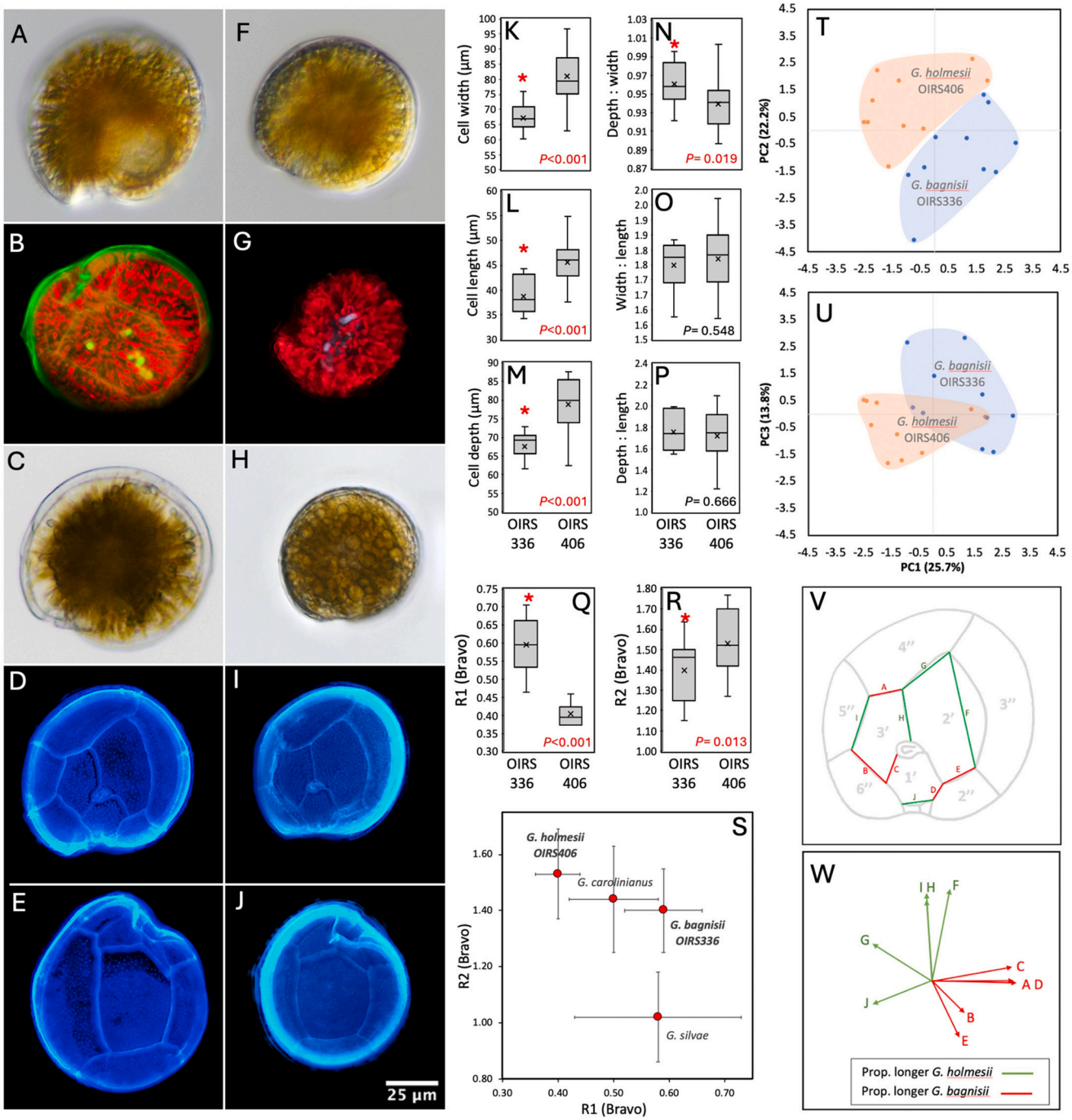

Fig. 2. A-W. Morphological and morphometric comparison of *G. bagnisii* sp. nov. OIRS336 with *G. holmesii* OIRS406 by light microscopy. **Figs. (A-E)**. *Gambierdiscus holmesii* OIRS406; (**Figs. F-J)**. *Gambierdiscus bagnisii* sp. nov. OIRS336. **A**. Apical view of *G. holmesii* (LM-IC) **B.** FM. Chlorophyll autofluorescence (FM) showing distribution of chloroplasts; **C)** Apical cross-section of *G. holmesii* (LM-BF) showing sparse distribution of chloroplasts in cell periphery. **D.** Apical view (FM) of calcoflour-stained epitheca of *G. holmesii*. **E)** Antapical view (FM) of calcoflour-stained hypothecal plates of *G. holmesii*. **F.** Apical view (LM-IC) of *G. bagnisii* sp. nov. OIR336. **G)** Chlorophyll autofluorescence (FM) showing distribution of chloroplasts; **H.** Apical cross-section of *G. bagnisii* (LM-BF) showing chloroplasts distributed throughout the cell. **I.** Apical view (FM) of calcoflour-stained epitheca of *G. bagnisii* sp. nov. OIRS336. **J.** Antapical view (FM) of calcoflour-stained hypothecal plates of *G. bagnisii* sp. nov. OIRS336. **K**—**P**. Cell size ranges and variance (width, depth, length, cell aspect ratios) of *G. bagnisii* sp. nov. OIRS336 and *G. holmesii* OIRS406. Range indicated by whiskers; mean indicated by X, *SD* indicated by grey boxes). Significantly different means (M) and p-value (ANOVA) indicated in red text. **Q-S**. Apical plate shape ratios R1 and R2 (Bravo et al., 2019) of *G. bagnisii* sp. nov. OIRS336 and *G. holmesii* OIRS406. **Q)** Mean and variance of R1 (rectangularity vs hatchet-shape 2′ plate). **R)** Mean and variance of R2 (eccentricity of P_o in apical plate series). Whiskers indicate range; cross indicates mean, grey box indicates upper/lower quartiles. Different means indicated by * and *p*-values (ANOVA) in red text. S) Comparison of R1 vs R2 ratios (mean ± SD) of *G. bagnisii* and *G. holmesii* compared to other species in the *G. polynesiensis* lineage. **T-W.** Morphometric analysis and comparison of apical and antapical plate series of *G. bagnisii* sp. nov. OIRS336 and *G. holmesii* OIRS406. **T-U.** Three-dimensional principal components analysis (PCA) of plate inter-junction distances showing clear separation of *G. bagnisii* sp. nov. OIRS336 from *G. holmesii* on the 1st and 2nd principal component axes. **V**—**W.** Major contributing of apical plate boundary measures (vectors, W) and their contribution to species separation on PC1 and PC2 axes (W).

rRNA, and 793 bp of the D8-D10 region of LSU rRNA. Single gene alignments were checked and concatenated using Geneious Prime 2023.2.1. Maximum likelihood (ML) analysis was performed using RAxML 8.2.11, with a GTR + G + I model, and 1000 bootstrap replicates. Bayesian phylogenetic analyses were performed using a GTR+ G + I model and was run until the standard deviation of split frequencies reached below threshold level. Chain length was 1,500,000 with a burnin of 500,000.

2.6. Scanning electron microscopy (SEM)

Cultures were sieved through a 50 μm mesh, resuspended in 5 mL media, preserved with 1 % Lugol's iodine. Cells were placed on a five μm Millipore filter, rinsed twice in distilled water, and dehydrated in a series of increasing ethanol concentrations (30, 50, 70, 85, 90, 100 %), followed by chemical drying with hexamethyldisilazane at room temperature. Samples were mounted and sputter coated with gold-palladium (SCD 050 Bal-Tec). Cells were observed using the SE detector of a Tescan VEGA3 microscope (Elekronen-Optik-Service GmbH, Dortmund, Germany) at 10 kV.

2.7. Toxin extraction

Gambierdiscus cells were extracted with 90 % aqueous methanol (sonication aided; 10 min at 59 kHz) at a ratio of one mL per 400,000 cells, followed by centrifugation (3200 xg, 10 °C for 10 min) and decanting. The process was repeated to provide a final extract concentration of 1 mL per 200,000 cells. Extracellular co-extractives were precipitated in the freezer (−20 °C) and clarified using centrifugation (3200 xg, 10 °C for 10 min) and an aliquot of the supernatant was transferred to a glass LC vial for analysis (Murray et al., 2018).

2.8. LC-MS

Analysis was performed on a Waters Xevo TQ-S triple quadrupole mass spectrometer coupled to a Waters Acquity UPLC i-Class. Chromatographic separation used a Waters Acquity UPLC BEH phenyl column (1.7 μm, 100 × 2 mm). CTX analogues were monitored in positive electrospray ionization (ESI) mode and the hydrophilic compounds (MTX-1, gambierones and gambieroxide) in negative ESI mode. Chromatographic separation was achieved on a Waters Acquity UPLC BEH phenyl column (1.7 μm, 100 × 2.1 mm), held at 50 °C, with mobile phases containing 0.2 % (*v*/*v*) of a 25 % NH_4OH solution in (A) Milli Q water and (B) 95 % aqueous MeCN (prepared fresh daily) and a flow rate of 0.55 mL/min. The injection volume was 2 μL and the autosampler chamber was held at 10 °C. The initial solvent composition was 5 % B, with a linear gradient to 50 % B from 1 to 3.5 min, a linear gradient to 75 % B from 3.5 to 7.5 min, ramped up to 95 % B by 8 min and held at 95 % B until 9 min, followed by a linear gradient back to 5 % B at 9.2 min. The column was then re-equilibrated with 5 % B for 0.8 min. The total injection time was 10 min. Mass spectrometer settings were: capillary voltage 3.0 kV, cone voltage 40 V, source temperature 150 °C, N2 gas desolvation flow rate 1000 L/h at 600 °C, cone gas 150 L/h, and the collision cell was operated with 0.15 mL/min argon. Data acquisition and processing were performed with MassLynx and TargetLynx software, respectively.

The isolates were analysed for six algal CTX analogues (CTX3B, CTX3C, M-seco-CTX3B/C, CTX4A, CTX4B, M-seco-CTX4A/B), gambierone, 44-methylgambierone and maitotoxin-1 using quantitation and confirmation multiple reaction monitoring (MRM) transitions that were experimentally determined using purified compounds or an algal extract (Table 1). The LoD was 1 ng/mL, which equates to 0.01 pg $cell^{-1}$ for culture extracts generated at a ratio of 200,000 cells mL^{-1}. The isolates were also qualitatively analysed for gambieroxide using a published MRM transition, and for a currently uncharacterized compound (1024 Da).

Calibrated reference material for CTX3B, CTX3C, CTX4A (Institute of Louis Malarde standards; 0–20 ng/mL), gambierone and 44-methylgambierone (44-MG) (in-house qNMR standards; 0–1000 ng/mL) was used for quantitation using five-point linear regression calibration curves ($R^2 > 0.98$). The calibration curves for CTX3B and CTX4A were used to quantify M-seco-CTX3B/C and M-seco-CTX4A/B, respectively, with a relative response factor of 1, and a CTX+ culture extract (*G. polynesiensis* CAWD212) was used to confirm elution time and confirmation ratio, including the uncharacterized compound (1024 Da). The presence of MTX-1 was confirmed using calibrated reference material (Wako standard) and a positive control culture (*G. australes* CAWD149).

2.9. Mouse bioassays

To determine the toxicity (LD_{50}) of culture extracts, the principles of OECD guideline 425 were followed. Female Swiss albino mice were bred at AgResearch, Ruakura, NZ. Mice were housed individually and were allowed unrestricted access to food and water. Experiments were approved by the Ruakura Animal Ethics Committee established under the Animal Protection (code of ethical conduct) Regulations Act., 1987

Table 1
List of the MRM transitions and CEs used to detect the metabolites.

Analogue	Chemical Formula	mw (Da) [a]	Precursor ion	MRM transition	CE (eV)	Retention time (min)
CTX4A/B	$C_{60}H_{84}O_{16}$	1060.6	$[M + H]^+$	1061.6 > 125.1 1061.6 > 155.1	50	7.05 and 7.25
M-seco-CTX4A/B	$C_{60}H_{86}O_{17}$	1078.6	$[M\text{-}H_2O + H]^+$	1061.6 > 125.1 1061.6 > 155.1	50	5.45
CTX-3B/C	$C_{57}H_{82}O_{16}$	1022.6	$[M + H]^+$	1023.6 > 125.1 1023.6 > 155.1	50	6.55 and 6.70
M-seco-CTX3B/C	$C_{57}H_{84}O_{17}$	1040.6	$[M\text{-}H_2O + H]^+$	1023.6 > 125.1 1023.6 > 155.1	50	4.75
MTX-1	$C_{164}H_{256}O_{68}S_2$	3379.6 [b]	$[M\text{-}2H]^{2-}$ $[M\text{-}3H]^{3-}$	1689.4 > 1689.4 1126.1 > 96.8	80 100	3.40
Gambierone	$C_{51}H_{76}O_{19}S$	1024.5	$[M\text{-}H]^-$ C-38 fragment	1023.3 > 96.8 899.2 > 96.8	50 50	3.00
44-MG	$C_{52}H_{78}O_{19}S$	1038.3	$[M\text{-}H]^-$ C-38 fragment	1037.3 > 96.8 899.2 > 96.8	70 50	3.10
Gambieroxide	$C_{60}H_{90}O_{22}S$	1194.6	$[M\text{-}H]^-$	1193.6 > 96.8	60	3.40
Unknown	–	1024.6	$[M + H]^+$	1025.6 > 157.1 1025.6 > 175.1	50	6.50

mw = Molecular weight; MRM = multiple reaction monitoring; CE = collision energy; CTX = ciguatoxin; MTX-1 = maitotoxin-1; 44-MG = 44-methylgambierone.
[a] Reported as the monoisotopic mass.

(New Zealand). Mice of 18–22 g were used and weighed immediately prior to dosing to allow the exact quantity of test compound required to be calculated. For intraperitoneal injection (i.p.) the dose was administered in 1 mL 1 % Tween in saline. For oral administration the dose was mixed with ground mouse food in a positive displacement pipette and applied over the tongue of the mouse. Mice were observed over the first 24 h for symptoms of toxicity. All survivors were retained for a 14-day observation and bodyweight and food intake measured regularly. At the completion mice were euthanized and weights of major organs recorded and expressed as the percentage of bodyweight.

2.10. Cell bioassay

Cell bioassay methods followed (Lewis et al., 2016). Briefly, SHSY5Y cells were plated into 384-well black walled imaging plates at a density of 50,000 cells per well and cultured for 48 h. Fluorescent responses (excitation, 470–495 nm; emission 515–575 nm) were assessed using the $FLIPR_{TETRA}$ after a 30 min incubation with a fluorescent Ca^{2+} dye (Calcium 4 No Wash Dye, Molecular Devices) diluted in PSS buffer containing 0.1 % BSA. Camera gain and intensity were adjusted so that each plate containing loaded cells yielded a minimum baseline fluorescence of 1200 arbitrary fluorescence units (AFU).

A two-addition protocol was used to determine activity of veratridine (1 μM - 45 μM), purified P-CTX-1 (6 fM - 10 nM) and fractionated OIRS extracts. After a 10 s baseline measurement was recorded, 10 μL of sample (Buffer/P-CTX-1 doses/OIRS fractions) was added to each well containing the loaded cells using a $FLIPR_{TETRA}$ injection manifold. Fluorescence was recorded every s for 300 s thereafter. A second addition (10 μL) of buffer (PSS) or varying concentrations of veratridine (1, 3 and 5 μM) followed by a further 300 reads (1 read/s) was used to determine synergistic effects on NaV activity.

To compute veratridine dose response, responses were normalized to baseline (read 1–10) and the maximum increase in fluorescence for reads 10–620 determined using ScreenWorks 3.2.0.14 (Molecular Devices). Similarly, to compute P-CTX-1 dose response at varying veratridine concentration, responses were normalized to baseline (read 310–320) and determine the maximum increase in fluorescence for reads 320–620. MTX-like activity was computed by normalizing the response to baseline (read 1–10), determining the maximum increase in fluorescence for reads 10–310 and plotted in Graphpad Prism by normalizing against the buffer control while CTX-like activity was computed after normalizing the response to baseline (read 310–320), determining the maximum increase in fluorescence for reads 320–620 and plotted in GraphPad Prism by normalizing against the 3 μM veratridine response.

3. Results

3.1. Morphological analysis

3.1.1. *Gambierdiscus bagnisii sp. nov.* (Figs. 2F-J, 3)

Cells were anterio-posteriorly compressed, lenticular, and round to oval from an apical view (Figs. 2F, H, I, 3B, C). Cells were 55–73 μm deep (M = 67.6, SD 4.66 μm, $n = 18$) and 60–76 μm wide (M = 67.1, SD 4.29 μm, n = 18) and 34–47 μm long (M = 38.8, SD 3.49 μm, $n = 14$) (Table 2, Figs. 2K-M). Cell depth to width ratio ranged from 0.92 to 1.00 (M = 0.96. SD 0.02 μm, n = 14); cell width to length ratio from 1.58 to 1.83 (M = 1.75, SD 0.09 μm, $n = 10$) (Table 2, Figs. 2N, O). Cell surface was smooth (apical plates and posterior intercalary plate) or foveate with shallow depressions (pre- and post-cingular, antapical plates) with irregularly scattered pores of two size classes (Fig. 3). Large pores had a diameter of 0.25–0.37 μm ($n = 20$) and small pores of 0.16–0.20 μm ($n = 15$). Wide intercalary bands were smooth or foveate (Figs. 3A-C, H-K), rarely slightly transversely striated (not shown). Plate formula (Kofoid tabulation) was P_o, 3′, 0a, 7″, 6c, 6 +?s, 5‴, 1p, 2‴“ (Figs. 3A-D, H-L). Apical pore plate (P_o) was teardrop shaped to triangular with a fish-hook shaped apical pore, shifted to the ventral side (Figs. 3B, C), about one third of the epitheca depth from the sulcus. P_o was 5.7–7.7 × 4.0–4.8 μm ($n = 11$) in size (Figs. 3B, C, E, F). Twenty-six to 39 large depressions/pores were distributed over the P_o plate ($n = 17$) and arranged in no consistent pattern (Figs. 3E, F); one row of depressions intruded into the hook, associated with additional depressions in the hook center. As seen by an inside view, the depressions contained a net-like ‘membrane’ with tiny pores (irregular in number and arrangement) (Fig. 3G). Two observed P_o plates had an additional small simple pore on its ventral side (Fig. 3G arrow). The largest apical plate was the hatchet-shaped 2′ plate (Figs. 3B-D). The suture 2′/2″ was about two thirds the length of the 2′/4″ suture (Table 2). The largest precingular plates were plate 3″ (four-sided, covering the left lateral precingular area) and the asymmetrical pentagonal 4″ plate (dorsal) (Figs. 3A-D). Plate 4″ had a longer 4″/2′ suture compared to the shorter 4″/3′ suture (Fig. 3C). In a few cases these sutures were nearly equal in length or the 4″/2′ suture was shorter (Fig. 3B). Plates 5″ and 6″ were on the right lateral to ventral side (Figs. 3B, C). Plates 1″ and 7″ were the smallest (Figs. 3A, D) located ventrally. A small fold on the 1″ plate was not always present (Figs. 3A, I). The largest postcingular plate was the pentagonal 4‴plate (covering most of the left lateral hypotheca margin), followed by the plates 2‴, 3‴, 5‴and 1‴(Figs. 3H-L). The pentagonal first antapical plate (1‴“) was small and the large, pentagonal 1p plate covered the antapex (Figs. 3H-L). Plate 1‴did not contact plate 1p (Figs. 3I, K, L). Plate 5‴did not contact plate 1p (Figs. 3H, J-L). The sulcus was deeply excavated

Table 2
Morphological features of clade III *Gambierdiscus* species, based on present study and (Chinain et al., 1999; Litaker et al., 2009; Jang et al., 2018; Fraga and Rodríguez, 2014).

Species	Thecal plate features		Apical Pore Complex (APC)		2′ plate shape		Cell dimensions		
	ornamentation	pores	displacement	eccentricity R1 M (range)	shape	hatchetness R2 M (range)	depth [μm]	Width [μm]	Depth:width ratio
G. bagnisii sp. nov.	smooth to foveate	2 size classes	ventral	0.59 (0.46–071)	hatchet	1.40 (1.15–1.63)	55.1–73.0	60.0–76.3	0.96 (0.92–1.00)
G. holmesii	smooth to foveate	1 size class	ventral	0.4 (0.37–0.52)	hatchet	1.53 (1.27–1.77)	60.8–88.9	63.1–97.0	0.94 (0.90–1.00)
G. silvae	differing intensity	2 size classes	slightly ventral	0.58 (0.24–0.96)	hatchet	1.02 (0.63–1.66)	69 ± 8	64 ± 9	
G. polynesiensis	smooth (to foveate*)	1 size class	ventral	0.64 (0.6 0–0.67)	hatchet	1.22 (1.18–1.25)	68.0–85.0	64.0–75.0	
G. carolinianus	smooth (to foveate*)	1 size class	ventral	0.50 (0.33–0.71)	hatchet	1.44 (1.02–1.90)	72.2–87.0	75.7–103.3	

(Figs. 3H-K), composed of six plus x plates. The narrow and deep cingulum was difficult to observe and consisted of 6 plates (not shown).

3.1.2. *Gambierdiscus holmesii (strain OIRS406)*

Strain OIRS406 conformed to the type description (Figs. 2A-E, Supplementary Figs. 1, 3A-D). Cells were 60 to 88 μm deep (M = 78.8, SD 7.21 μm, $n = 25$), 63–97 μm wide (M = 80.9, SD 7.40 μm), and from 32 to 52 μm long (M = 45.6, SD 4.12 μm, $n = 34$) (Table 2, Fig. 2). The depth to width ratio of cells ranged from 0.90 to 1.00 (M = 0.94 (SD 0.03 μm, n = 25); the cell width to length ratio ranged from 1.57 to 1.97 (M = 1.77, SD 0.10 μm, $n = 30$) (Table 2, Fig. 2). P_o was approximately 7.2–7.9 × 4.4–5.4 μm in size ($n = 8$) (Supplementary Figs. 1E-G). Twenty-one to 42 large depressions/pores ($n = 12$) were distributed over the P_o plate (Supplementary Figs. 1E-G). Only large thecal pores, 0.22–0.33 μm in diameter ($n = 20$), were observed (Supplementary Fig. 1N).

3.2. Morphological comparison of *G. bagnisii* sp. nov. with *G. holmesii*

Cultured cells of *G. bagnisii* sp. nov. OIRS336 and *G. holmesii* OIRS406 had similar gross morphology (Fig. 2); a smooth to foveate theca with limited ornamentation or reticulation, similar shape with similar cells aspect ratio, and identical apical and antapical plate patterns. Despite overlap of cell size ranges, *G. bagnisii* cells were significantly smaller than *G. holmesii* (Fig. 2 K—N). Cultured under identical conditions, *G. holmesii* could be distinguished from *G. bagnisii* cells using bright field illumination due to the sparse distribution of chloroplasts in the cell periphery, compared to evenly distributed chloroplasts in *G. bagnisii* (Figs. 2C, H). The shape of apical and antapical plates showed considerable individual variation (Figs. 2D-J). Morphometric multivariate analysis (PCA) of apical and antapical plate series (Figs. 2T, U) resolved two distinct species clusters primarily from consistent differences in apical plate series shapes (Figs. 2V, W). These differences were partially captured by differences in plate ratios R1 and R2 (Bravo et al., 2019) that respectively measure squareness of 2′ plate, and eccentricity of P_o within the apical plate series (Figs. 2Q-S). Comparison of R1 and R2 also distinguished *G. bagnisii* from *G. silvae*, a similar-sized smooth-theca species in the *G. polynesiensis* lineage (Fig. 2S).

3.3. Phylogenetic analyses

Maximum likelihood phylogenies from concatenated rRNA regions (4154 bp, Fig. 4A) and those conducted with Bayesian analysis had the same topology, with strong support for the major clades of *Gambierdiscus,* with *Fukuyoa* as a sister group. Within Clade III, the grouping of *G. holmesii*, *G. bagnisii*, *G. silvae*, *G. polynesiensis* and *Gambierdiscus* sp. 3 was fully supported, and the clade of the first four of these taxa was strongly supported (96/0.99 BS/PP, Fig. 4A). A clade comprising *G. holmesii*, *G. bagnisii*, *G. silvae* was fully supported, with *G. silvae* positioned as the fully supported outgroup to the other two. The three strains of *G. holmesii* from the northern and southern GBR as a single clade received moderate support (62/0.85 BS/PP, Fig. 4A), with *G. bagnisii* as the sister taxon. Analysis of 20 single copy transcripts common to the 6 *Gambierdiscus* species and *Ostreopsis* outgroup taxa (Fig. 4B) supported a clade of *G. holmesii*, *G. bagnisii* and *G. polynesiensis*. Grouping of *G. holmesii* with *G. bagnisii* was highly supported (Fig. 4B, 94/1.00 BS/PP). Analyses of the D8-D10 LSU rRNA, grouped *G. bagnisii* with sequences of *Gambierdiscus* sp. 4 from Kiribati (Supplementary Fig. 5), outside *G. silvae* and *G. holmesii*. Pairwise identity from aligned single gene regions of *G. holmesii* and *G. bagnisii* showed a similarities of 97.7 %, 99.0 %, 99.3 % and 98.9 % for ITS1/5.8S/ITS2 (290 bp), LSU rDNA regions D1-D3 (902 bp), D8-D10 (736 bp), and SSU rDNA (1540 bp), respectively (Supplementary Table 2).

3.4. Toxin analysis

G. holmesii OIRS 406 produced M-seco-CTX4A/B (Fig. 4C; Table 1, identified based on the same retention time and MRM confirmation ratio as the reference material), with a cell quota, quantified using CTX4A, of 0.05 pg cell^{-1} (range 0.04–0.06 pg cell^{-1}) (Fig. 4C). Isolates of *G. polynesiensis*, CAWD212 and CAWD267, had M-seco-CTX4A/B cell quotas of 1.3 and 2.0 pg cell^{-1}, respectively (Fig. 4C). The toxicity of M-seco-CTX4A/B is unknown. *Gambierdiscus bagnisii* sp. nov. OIRS 336 and *G. holmesii* OIRS 406 also produced an uncharacterised compound (1024 Da), previously detected only from *G. polynesiensis*, at cell quotas of 0.1–4.0 pg cell^{-1} when quantified using CTX3C (Fig. 4C). It is unknown if this compound is toxic and of any relevance to CP. *Gambierdiscus bagnisii* sp. nov. OIRS 336 produced a mean of 7 pg cell^{-1} of gambierone and 30 pg cell^{-1} of 44-methylgambierone, but no maitotoxin 1 was detected, while *G. holmesii* OIRS 406 produced a mean of 0.8 pg cell^{-1} of gambierone and 6.25 pg cell^{-1} of 44-methylgambierone, but no maitotoxin 1 was detected.

3.5. Mouse bioassay

Gambierdiscus bagnisii (OIRS 336) extracts were toxic to mice by IP injection with an LD_{50} of 1.39 mg/kg (confidence intervals 1.21–1.66 mg/kg) (Fig. 4F). In terms of extracted cell numbers the LD_{50} was 239,224 cells/kg (confidence intervals 208,245–285,691 cells/kg) (Fig. 4F). Symptoms of toxicity were abdominal stretching with ears back, head down and orbital tightening. At lethal doses slow or jerky movement and slowing respiration were observed. If laboured breathing was observed mice were euthanized. No abnormalities were observed at necropsy and the weights of the major organs in percentage of body-weight were within normal limits. These signs of toxicity did not include lachrymation or hypersalivation, characteristic effects seen in mice dosed with P-CTXs and extracts of *G. polynesiensis* (Fig. 4F). The LD_{50} of *Gambierdiscus holmesii* OIRS 406 was 1.39 mg/kg (1.21–2.66 mg/kg) by extract weight and 70,604 cells/kg (61,461 and 84,318) by the cell number extracted (Fig. 4F). Symptoms of toxicity were analogous to those observed in mice dosed with *Gambierdiscus bagnisii* OIRS 336 extracts. No oral toxicity of OIRS 336 or OIRS 406 extracts was observed at dose rates of up to 500 mg/kg.

3.6. Cell bioassay

HPLC-fractionated extracts of *G. holmesii*, *G. bagnisii* sp. nov. and *G. polynesiensis* CAWD267 were assessed for MTX-like and CTX-like activity using an SH-SY5Y bioassay (Lewis et al., 2016). Maitotoxin-like activity was identified in all three species, potentially with multiple variants, while later eluting CTX-like activity was only clearly identified in *G. polynesiensis* (Fig. 4G).

3.7. Metabarcoding analyses of the GBR and wider species distribution

Using metabarcoding of the V4 region of SSU rDNA, *Gambierdiscus bagnisii* was detected from Beaver Reef and Orpheus Island (Fig. 5A). *Gambierdiscus holmesii* was detected from all sites at Heron Island and Beaver Reef and some sites from Orpheus Island (Fig. 5A). *Gambierdiscus polynesiensis* was detected in the majority of samples at all locations in the GBR (Beaver Reef, Orpheus Island and Heron Island) (Fig. 5A). The identification of ASVs from metabarcoding was confirmed using phylogenetic analysis of ASVs (Supplementary Fig. 6), which showed well supported clades of ASVs with SSU rDNA sequences from well-studied or reference strains of the relevant species.

G. polynesiensis has been detected from the Cook Islands, the Kingdom of Tonga, and certain islands in French Polynesia (Fig. 5B). The

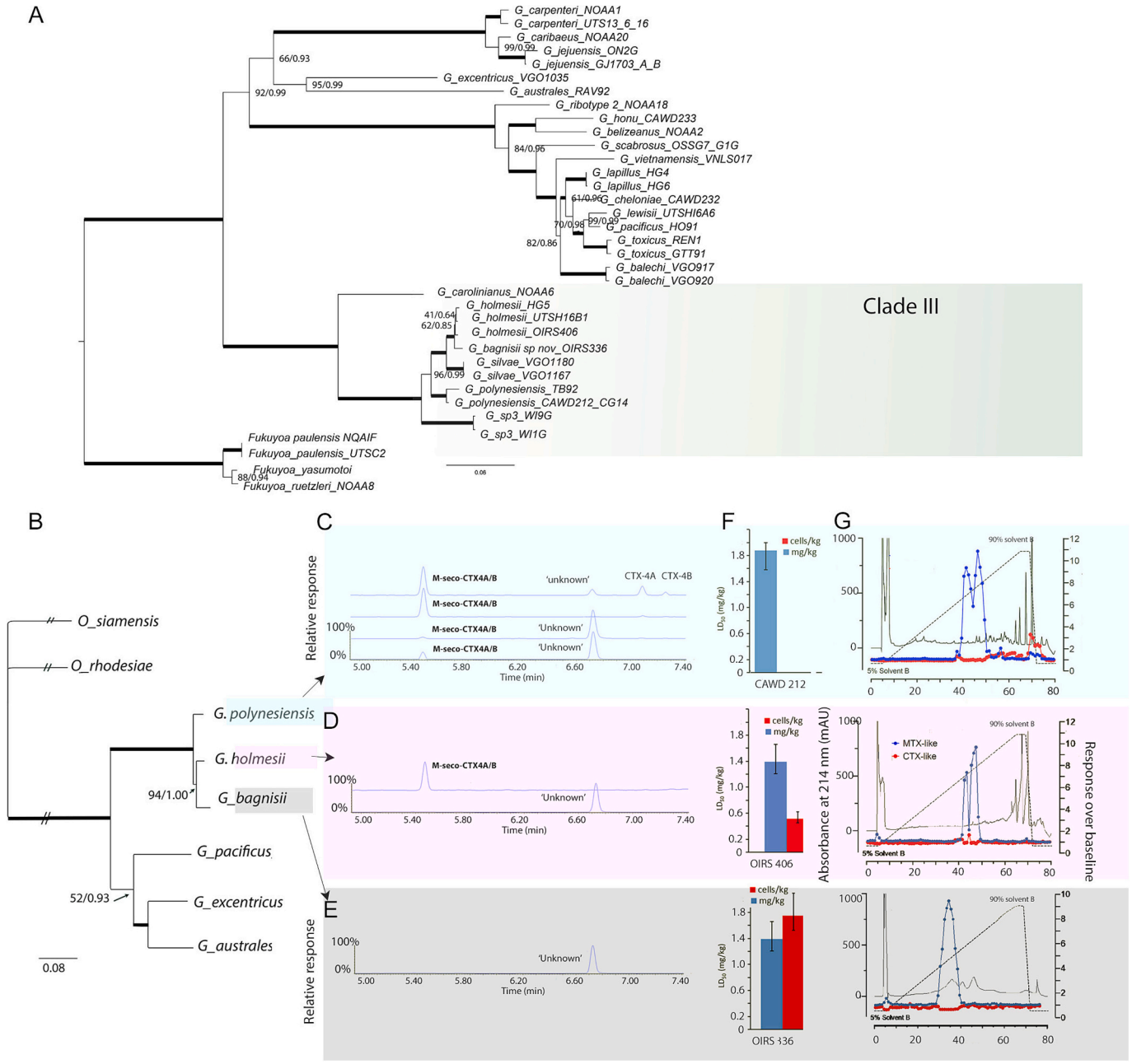

Fig. 4. **A**. Phylogeny of *Gambierdiscus* strains, based on most likely tree showing Maximum likelihood (ML) and Bayesian analyses (BA) of a concatenated alignment of 3940 bp of 18S, ITS1–5.8S-ITS2, 28S D1-D3 and D8-D10 rRNA including the new species *G. bagnisii* (NCBI accession: PQ453126, PQ453127, PQ464796, PQ464797, PQ467097, PQ467098, PQ464793, PQ464794). Values at the nodes represent ML bootstrap and BA posterior probability support. Thick black lines represent full support. Scale bar is substitutions per site. **B**. Phylogeny based on most likely tree showing Maximum likelihood (ML) and Bayesian analyses (BA) from a concatenated alignment of 20 homologous single copy nucleotide transcripts (20,626 bp). Transcripts were extracted from 6 *Gambierdiscus* species and two outgroups (*Ostreopsis* spp). **C.** Extracted ion chromatograms showing M-seco-CTX4A/B in (in descending order) *G. polynesiensis* CAWD212, *G. polynesiensis* CAWD267, and an 'unknown' analogue (*m/z* 1025) observed in *G. polynesiensis* CAWD212, *G. polynesiensis* CAWD267 **D.** Extracted ion chromatograms showing M-seco-CTX4A/B in *G. holmesii* OIRS406, and an 'unknown' analogue (m/z 1025) in *G. holmesii* OIRS406, **E.** An 'unknown' analogue (m/z 1025) in *G. bagnisii* OIRS336. **F**. Toxicity by IP injection of extracts from *G. holmesii* OIRS406, *G. bagnisii* OIRS 336 and *G. polynesiensis* CAWD212. **G.** Results of the SH-SY5Y cell bioassay on *G. holmesii* OIRS406, *G. bagnisii* OIRS 336 and *G. polynesiensis* CAWD267.

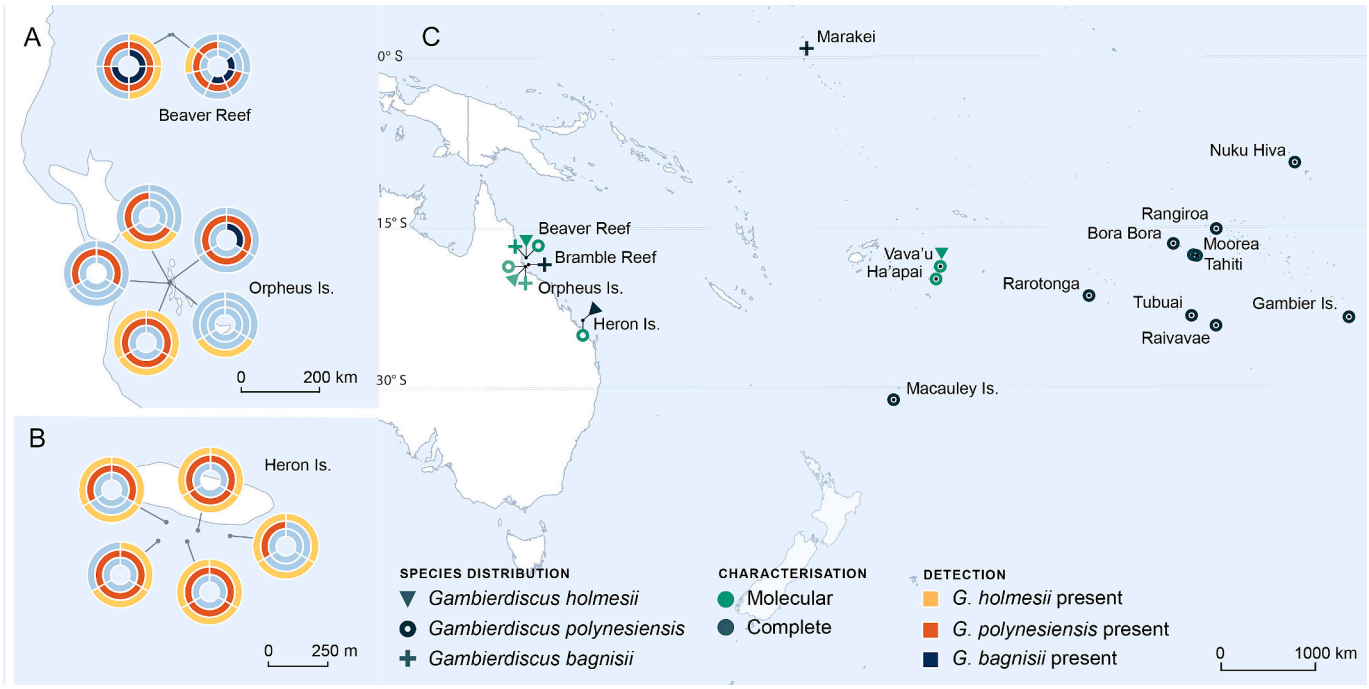

Fig. 5. A. Distribution of *Gambierdiscus polynesiensis*, *G. holmesii* and *G. bagnisii* sp. nov. from samples from sites in the Great Barrier Reef: Beaver Reef. Donut plots show number of positive detections from replicate samples collected from multiple sites. Colour sections represent positive detections and blue sections represent no detection. Orpheus Island and Heron Island from analyses of high-throughput sequencing metabarcoding analyses of the V4 region of SSU rRNA. **B.** Distribution of *Gambierdiscus polynesiensis*, *G. holmesii* and *G. bagnisii* on Heron Island. **C.** Currently known distribution of *Gambierdiscus polynesiensis*, *G. holmesii* and *G. bagnisii* from the South Pacific region, including both fully characterised reports (isolation of cultures with associated DNA sequences) and molecular detection only reports (high-throughput sequencing metabarcoding and quantitative PCR studies). Information for Macauley Island (Rangitāhua/NZ) (Rhodes et al., 2017)), Marakei (Kiribati), (Xu et al., 2014b), Vava'u and Ha'apai (Kingdom of Tonga) (Argyle et al., 2023), Rarotonga (Cook Islands), (Rhodes et al., 2014), Nuku Hiva, Bora Bora, Moorea, Tahiti, Tubuai, Gambier Islands, Rangiroa, Raivavae (French Polynesia) (Chinain et al., 2023).

most southern occurrence of this species is Macauley Island, part of the Rangitāhua/Kermadec Islands, an uninhabited territory of Aotearoa New Zealand (Fig. 5B and references therein). *Gambierdiscus holmesii* has been found in the GBR and the Kingdom of Tonga, while *G. bagnisii* has been previously found (as *Gambierdiscus* sp. 4) from Marakei (Republic of Kiribati) in the central Pacific (Fig. 5B and references therein).

4. Discussion

4.1. Clade III *Gambierdiscus* and CTXs in GBR and South Pacific coral reef food webs

CP is an emerging issue in the context of 'planetary health', due to its increasing impacts on human health in relation to marine ecosystem disruption (Kohli et al., 2014; Tester et al., 2010; Rongo and Van Woesik, 2013; Chateau-Degat et al., 2005; Kibler et al., 2015; Farrell et al., 2017). Despite this, the prediction and monitoring of CP is not well developed anywhere in the world (Chinain et al., 2021; *Report.*, 2018). Australia has experienced >1700 reported CP cases including two deaths (from 1965 to 2020 (Tonge et al., 1967; Hamilton et al., 2010), Fig. 1C), yet predictive management has been greatly hindered because the identity of CTX-producing *Gambierdiscus* spp. has remained unclear, as it has in many other countries. This lack of knowledge internationally is reflective of both the difficulty in isolating and identifying *Gambierdiscus* taxa and its CTXs and the low level of resourcing for researching a tropical illness largely impacting the Global South. The South Pacific Ocean is the location of the majority of the world's annual reported CP cases (Supplementary Table 1), yet to date, confirmed CTX-producing *Gambierdiscus* taxa via LC-MS are only known from three inhabited nations (Chinain et al., 2010; Rhodes et al., 2014; Argyle et al., 2023). Here, we show the presence of *G. polynesiensis* and *G. holmesii,* two closely related (Clade III) species of *Gambierdiscus* (Fig. 5A) distributed in the far north to southern GBR, Australia (Figs. 5A, from 18.6°S - 23.4°S), and elsewhere in the South Pacific (Fig. 5C). *G. polynesiensis* and *G. holmesii* produce chemically detectable analogues of CTXs (Fig. 4 C, D, E), the first confirmed report of an algal CTX analogue produced by a species other than *G. polynesiensis*.

Prior to this study, no identified *Gambierdiscus* (Murray et al., 2014; Kohli et al., 2014; Sparrow et al., 2017; Kretzschmar et al., 2017; Kretzschmar et al., 2019; Larsson et al., 2018) in Australia had been confirmed to produce chemically detectable CTXs, specifically analogues that bioconvert to the highly toxic fish metabolites CTX1B, 52-epi-54-deoxy CTX1B, 54-deoxy CTX1B (Ikehara et al., 2017; Yogi et al., 2014), which are common in the region. An unidentified strain of *Gambierdiscus* (WC 1/1) from southern QLD (Fraser Island, 25°S) isolated in 1991 produced chemically detectable levels of a less polar CTX (Lewis and Endean, 1984; Kohli et al., 2017; Holmes and Lewis, 1994), but the strain was lost prior to further research. Of known *Gambierdiscus* species in the GBR (*G. carpenteri*, *G. honu*, *G. holmesii*, *G. lapillus*, *G. lewisii*, and *F. paulensis*, (Murray et al., 2014; Kohli et al., 2014; Sparrow et al., 2017; Kretzschmar et al., 2017; Kretzschmar et al., 2019; Larsson et al., 2018)), the few detections of CTX-like activity, via bioassays, in strains of these species isolated from the Caribbean and/or Pacific have been low (< 0.015 pg cell^{-1}) or not quantifiable (Lewis et al., 2016; Holland et al., 2013). Here we have shown that *G. holmesii* produced 0.04–0.06 M-seco-CTX4 A/B pg cell^{-1}, and *G. polynesiensis* produced 1.3 and 2.0 M-seco-CTX4 A/B pg cell^{-1}. Previous reports of CTXs produced by *G. polynesiensis* strains isolated from other localities in the South Pacific have differed from one another in toxin quotas, with a mean for *G. polynesiensis* of 5.15 pg cell^{-1} CTX3C, —3B, −4 A, —4B (Chinain et al., 2010; Rhodes et al., 2014; Longo et al., 2019a; Munday et al., 2017; Longo et al., 2019b).

There are several factors that influence whether a *Gambierdiscus* species is likely to be an important source of CTX toxins in fish in a

region. These are: 1) the production of sufficient concentrations of analogues of CTXs that bioconvert to the analogues in local fish; 2) a wide distribution in the region; and 3) an environmental abundance above a threshold amount. Based on chemically detectable CTX production (Fig. 4 C-G) and widespread distribution (Fig. 5C), we propose that Clade III *Gambierdiscus,* particularly *G. polynesiensis,* are the primary human food chain source of CTXs in the South Pacific region. Previously, *G. australes* and *G. pacificus* have been considered to contribute to CP in the Pacific (Chinain et al., 2021), as they are widely distributed, can be common and abundant (Tester et al., 2020), and have shown CTX-like activity using the receptor binding assay, mouse bioassay, and the neuroblastoma cell-based assay (Hoppenrath et al., 2023; Pisapia et al., 2017). However, confirmed CTX compounds have not been found from strains from the Pacific region of these taxa using LC-MS/MS (Rhodes et al., 2014; Munday et al., 2017), indicating that the CTX cell^{-1} produced, if any, is lower than chemical detection thresholds.

CTX toxin cell quotas of *G. polynesiensis* strains cultured to date (ie mean cell toxin quota = 5.15 pg cell^{-1} CTX3C, —3B, −4 A, —4B (Chinain et al., 2010; Rhodes et al., 2014; Longo et al., 2019a; Munday et al., 2017; Longo et al., 2019b)) are from at least 2–5 orders of magnitude higher than other *Gambierdiscus* species cultured from the region, including *G. australes* from the Pacific (Chinain et al., 2010; Rhodes et al., 2014; Pisapia et al., 2017; Kohli et al., 2015). CTXs both accumulate and are eliminated from fish at certain rates (Clausing et al., 2018), with one study showing the majority of CTXs fed to fish were eliminated within 24 h (Ledreux et al., 2014). Fish eat a limited amount of biomass each day [ie 58], while *Gambierdiscus* species are most frequently present at abundances of 1–1000 cells g^{-1} wet weight algae (Litaker et al., 2010). If a *Gambierdiscus* species has a CTX toxin cell quota 2–5 orders of magnitude lower than that of a very toxic CTX producer, CTXs may never accumulate enough in fish to concentrations high enough to be chemically detected, because they may be eliminated faster than the fish are able to eat algal biomass containing sufficient *Gambierdiscus* cells.

On the other hand, if a species of *Gambierdiscus* produces CTXs at a concentration of 2–5 orders of magnitude higher, it may lead to uptake of CTXs in fish even if it forms <5 % of the *Gambierdiscus* assemblage in the area. As few as ~2 cells^{-1} cm^2 of *G. polynesiensis* on mesh screens were sufficient for CTXs to be detected in local herbivorous fish with a small home range (*Ctenochaetus striatus*), in a study of the Cook Islands (Smith et al., 2023). Other *Gambierdiscus* spp.: *G. pacificus*, *G. australes*, *G. honu*, *G. carpenteri*, *G. toxicus*, *G. cheloniae* were much more abundant than *G. polynesiensis*, which made up only 0.7–6 % of the *Gambierdiscus* assemblage in that study (Smith et al., 2023), but their presence was not correlated with CTXs in local fish (Smith et al., 2023). Experimentally, the provision of 89 *G. polynesiensis* cells g^{-1} fish daily (i.e., 8900 cells day^{-1} per 100 g fish) led to CTX1B concentration in fish above the regulatory limit for food safety after two weeks (Clausing et al., 2018). Considering a *C. striatus* feeding rate of 7200–12,600 bites day^{-1} (Holmes and Lewis, 2023), this appears enough to account for the accumulation of CTX in the marine food web at an abundance of ~2 cells^{-1} cm^2 of *G. polynesiensis* on macro-algal thallus. Feeding studies using low-toxin-producing *Gambierdiscus* species would be required in order to confirm or otherwise this hypothesis.

Such a low concentration of two cells^{-1} cm^2 of epiphytic microalgae could be overlooked using common sampling approaches, such as macroalgal or deployed screen rinsing, and light microscope observation and culture. *Gambierdiscus* concentrations in general are often relatively low, with at least 35 % of samples from the Pacific Ocean region showing cell abundances <10 cells g^{-1} of wet weight algae (Litaker et al., 2010). Hence, this may be one of the reasons why *G. polynesiensis* or a close Clade III relative are known to occur in so few South Pacific nations with CP (Fig. 5C). Sampling methods appropriate for identifying rare and cryptic marine benthic microbial species: metabarcoding, qPCR, and other sensitive molecular genetic approaches, may be important to ensuring that potential CTX- producing species are not overlooked. Additionally, long term studies or studies involving multiple sites may be necessary to document a more comprehensive benthic dinoflagellate community in a region.

4.2. *Gambierdiscus* Clade III morphological and phylogenetic relatedness

We describe a new, closely related species, *G. bagnisii* sp. nov., a member of the *Gambierdiscus* Clade III. While no single morphological feature clearly distinguishes *Gambierdiscus bagnisii* sp. nov. from sister species in clade III (Table 2), a combined analysis of morphometrics and thecal plates (Fig. 2) were able to distinguish *G. bagnisii* from sister species (Kretzschmar et al., 2019; Fraga and Rodríguez, 2014; Table 2). To distinguish species of *Gambierdiscus* with certainty, molecular genetic analysis is necessary (Figs. 4, Supplementary Table 2, Supplementary Figs. 5, 6). *G.bagnisii* sp. nov. has been previously reported from Kiribati in the central Pacific, as *Gambierdiscus* sp. 4 (Xu et al., 2014a), and our strain from the GBR showed extremely high genetic similarity to these strains (Supplementary Fig. 5). Our phylogenetic analysis of a concatenated region of rRNA (Fig. 4A) and the large alignment of 20 nuclear single copy genes (Fig. 4B) shows the close relationship between members of Clade III *Gambierdiscus*, specifically *Gambierdiscus polynesiensis*, *G. silvae*, *G. holmesii* and *G. bagnisii* sp. nov.

Our analyses show that *G. bagnisii* does not produce known CTXs (Figs. 4 C-G). The mouse bioassay results showed a lower oral toxicity of *G. holmesii* and *G. bagnisii* sp. nov. compared to *G. polynesiensis* (Fig. 4F), suggesting that *G. bagnisii* sp. nov. is unlikely to be involved in CP. All three species produced an uncharacterised compound, which to our knowledge has not been found from strains of any other *Gambierdiscus* species analysed to date (Fig. 4 C, D, E; JS Murray, unpublished data). The characterization of the unknown compound, found in all three species including determining the bioactivity and relative toxicity, is essential to determining if they pose a risk to human health. Such chemical analyses are needed to determine if other toxic compounds are potentially produced by *G. bagnisii* sp. nov. and *G. holmesii,* and if so, whether they may contribute to CP.

4.3. Conclusion

Most of the world's disease burden of CP occurs in the South Pacific, yet little is known about causative taxa producing CTXs in the region. Here, we have shown the presence and abundance of *G. polynesiensis* in locations of the far northern to southern GBR (~1000 km). This species and the closely related *G. holmesii,* also common in the GBR, produced a chemically detectable CTX analogue, suggesting they may be the main source of CTXs in marine food webs in the South Pacific Ocean. A new closely related species, *G. bagnisii* sp. nov., previously known from Kiribati as G. sp. 4, produced an as yet uncharacterised compound, however, it is unknown if it is toxic and of interest. Methods suitable for the detection of rare marine epiphytic microbes may be key to understanding causative agents of CP. Given predicted climate change related CP increases, efforts to reduce public health burdens will greatly benefit from targeted monitoring of *Gambierdiscus* species.

5. Taxonomic treatment

5.1. *Gambierdiscus bagnisii sp. nov.*

5.1.1. Description

Cells anterioposteriorly compressed, round to oval, lenticular. Cell depth 55–73 μm, cell width 60–76 μm; cell length 34–47 μm. Smooth or foveate thecal ornamentation with scattered pores of two size classes. Intercalary bands smooth or foveate. Thecal tabulation: APC 3′ 0a 7″ 6c 6 s? 5‴1p 2‴‘. APC shifted to the ventral side, about one third of the epitheca depth from the sulcus. P_o size: 5.7-7.7 x 4.0-4.8 μm. Hatchet-shaped 2’ plate. 2’/2” suture about half the length of 2′/4″ suture. Plate 4″ with longer 4″/2′ suture compared to the shorter 4″/3′ suture.

Large, pentagonal 1p plate. Plates 1‴and 5‴not contacting plate 1p.

5.1.2. Etymology

The species is named after Raymond Bagnis, pioneer researcher on Ciguatera Poisoning.

5.1.3. Holotype

Fig. 3C (OIRS 336); SEM-stub (CEDiT2024H182) deposited at Senckenberg am Meer, German Centre for Marine Biodiversity Research, Centre of Excellence for Dinophyte Taxonomy, Germany.

5.1.4. Isotype

Lugol's-fixed subsample of strain OIRS 336 (CEDiT2024I183) deposited at Senckenberg am Meer, German Centre for Marine Biodiversity Research, Centre of Excellence for Dinophyte Taxonomy, Germany.

5.1.5. Molecular diagnosis

Strain OIRS 336; partial SSU (PQ453126), ITS1/5.8S/ITS2 (PQ464796), LSU D1-D3 (PQ467097) and LSU D8-D10 (PQ464793).

5.1.6. Type locality

Eastern Orpheus Island (18° 36′ S, 146° 30′ E), Great Barrier Reef, Australia.

5.1.7. Molecular characterization

Gambierdiscus bagnisii sp. nov. can be genetically identified by rDNA sequences deposited in GenBank SSU: PQ453126.

Supplementary data to this article can be found online at https://doi.org/10.1016/j.scitotenv.2025.179990.

CRediT authorship contribution statement

Shauna A. Murray: Writing – review & editing, Writing – original draft, Supervision, Resources, Project administration, Methodology, Investigation, Funding acquisition, Formal analysis, Conceptualization. **Arjun Verma:** Investigation, Formal analysis. **Mona Hoppenrath:** Writing – original draft, Investigation, Formal analysis. **D. Tim Harwood:** Writing – review & editing, Investigation, Formal analysis. **J. Sam Murray:** Writing – review & editing, Investigation, Formal analysis. **Kirsty F. Smith:** Writing – review & editing, Investigation, Formal analysis. **Richard Lewis:** Writing – review & editing, Investigation, Formal analysis. **Sarah C. Finch:** Writing – review & editing, Investigation, Formal analysis. **Shikder Saiful Islam:** Writing – review & editing, Investigation, Formal analysis. **Amna Ashfaq:** Writing – review & editing, Investigation, Formal analysis. **Caroline Dornelles De Azevedo:** Writing – review & editing, Investigation, Formal analysis. **Christopher J.S. Bolch:** Writing – review & editing, Writing – original draft, Supervision, Resources, Investigation, Funding acquisition, Formal analysis, Conceptualization.

Permits

Samples were collected under GBRMPA permit G20/44763.1 in relation to project “The diversity, ecology, evolution and toxicology of ciguatera related dinoflagellates”.

Funding

This work was supported by the Australian Research Council (LP1800001) to SM, CB, TH, RL. The Hanse Wissenschaftskolleg (Delmenhorst, Germany) are thanked for providing SM with a fellowship while this manuscript was written.

Declaration of competing interest

The authors declare the following financial interests/personal relationships which may be considered as potential competing interests: Shauna Murray, Christopher Bolch, Tim Harwood reports financial support was provided by Australian Research Council. If there are other authors, they declare that they have no known competing financial interests or personal relationships that could have appeared to influence the work reported in this paper.

Acknowledgements

We acknowledge funding from the Australian Government's ARC Linkage scheme (LP1800001), and the assistance of staff at the Orpheus Island research station. We thank Matt Tesoreiro for assisting with Orpheus Island field collection, Marisol Lenzen for assistance, Javier Perez Burillo for preparing Fig. 1 and Jacqui Stuart for Fig. 5.

Data availability

Data will be made available on request.

References

Anderson, M.J., Gorley, R.N., Clarke, K.R., 2008. Permanova+ for Primer: Guide to Software and Statistical Methods. Primer-E, Plymouth, UK.
Argyle, P.A., Rhodes, L.L., Smith, K.F., et al., 2023. Diversity and distribution of benthic dinoflagellates in Tonga include the potentially harmful genera *Gambierdiscus* and *Fukuyoa*. Harmful Algae 130, 102524.
Bell, J.D., Ganachaud, A., Gehrke, P.C., et al., 2013. Mixed responses of tropical Pacific fisheries and aquaculture to climate change. Nat. Clim. Chang. 3, 591–599.
Bolger, A.M., Lohse, M., Usadel, B., 2014. Trimmomatic, a flexible trimmer for illumina sequencing data. Bioinformatics 30, 2114–2120.
Bravo, I., Rodriguez, F., Ramilo, I., et al., 2019. Ciguatera-causing dinoflagellate *Gambierdiscus* spp. (Dinophyceae) in a subtropical region of North Atlantic Ocean (canary islands): morphological characterization and biogeography. Toxins 11.
Callahan, B., McMurdie, P., Rosen, M., et al., 2016. Dada2: high resolution sample inference from illumina amplicon data. Nat. Methods 13, 581–583.
Chateau-Degat, M.L., Chinain, M., Cerf, N., et al., 2005. Seawater temperature, *Gambierdiscus* spp. variability and incidence of ciguatera poisoning in French Polynesia. Harmful Algae 4, 1053–1062.
Chinain, M., Faust, M.A., Pauillac, S., 1999. Morphology and molecular analyses of three toxic species of *Gambierdiscus* (Dinophyceae): *G. pacificus* sp. nov., *G. australes* sp. nov, and *G. polynesiensis* sp. nov. J. Phycol. 35, 1282–1296.
Chinain, M., Darius, H.T., Ung, A., et al., 2010. Growth and toxin production in the ciguatera-causing dinoflagellate *Gambierdiscus polynesiensis* (Dinophyceae) in culture. Toxicon 56, 739–750.
Chinain, M., Gatti, C.M.I., Darius, H.T., et al., 2021. Ciguatera poisonings: a global review of occurrences and trends. Harmful Algae 102, 101873.
Chinain, M., Gatti Howell, C., Roué, M., et al., 2023. Ciguatera poisoning in French Polynesia: a review of the distribution and toxicity of *Gambierdiscus* spp., and related impacts on food web components and human health. Harmful Algae 129, 102525.
Clausing, R.J., Losen, B., Oberhaensli, F.R., et al., 2018. Experimental evidence of dietary ciguatoxin accumulation in an herbivorous coral reef fish. Aquat. Toxicol. 200, 257–265.
Farrell, H., Harwood, D.T., Murray, S.A., 2016. Is ciguatera moving south in Australia? Harmful Algae News. 54, 5–6.
Farrell, H., Murray, S.A., Zammit, A., et al., 2017. Management of Ciguatoxin risk in eastern Australia. Toxins 9.
Fraga, S., Rodríguez, F., 2014. Genus *Gambierdiscus* in the canary islands with description of *Gambierdiscus silvae* sp. nov., a new potentially toxic epiphytic benthic dinoflagellate. Protist 165, 839–853.
Friedman, M.A., Fernandez, M., Backer, L.C., et al., 2017. An updated review of ciguatera fish poisoning: clinical, epidemiological, environmental, and public health management. Mar. Drugs 15.
Fritz, L., Triemer, R.E., 1985. A rapid simple technique utilising calcofluor white M2r for the visualisation of dinoflagellate thecal plates. J. Phycol. 21, 662–664.
Gillespie, N.C., Lewis, R.J., Pearn, J.H., et al., 1986. Ciguatera in Australia: occurrence, clinical features, pathophysiology and management. Med. J. Aust. 145, 584–590.
Guillard, R., Hargraves, P., 1993. *Stichochrysis immobilis* is a diatom, not a chrysophyte. Phycologia 32, 234–236.
Haas, B.J., Papanicolaou, A., Yassour, M., 2013. De novo transcript sequence reconstruction from RNA-seq using the trinity platform for reference generation and analysis. Nat. Protoc. 8, 1494–1512.
Hamilton, B., Whittle, N., Shaw, G., et al., 2010. Human fatality associated with Pacific Ciguatoxin contaminated fish. Toxicon 56, 668–673.
Hirama, M., Oishi, T., Uehara, H., et al., 2001. Total synthesis of Ciguatoxin CTX3c. Science 294, 1904–1907.

Holland, W.C., Litaker, R.W., Tomas, C.R., et al., 2013. Differences in the toxicity of six *Gambierdiscus* (Dinophyceae) species measured using an in vitro human erythrocyte lysis assay. Toxicon 65, 15–33.
Holmes, M.J., Lewis, R.J., 1994. Purification and characterisation of large and small maitotoxins from cultured *Gambierdiscus toxicus*. Nat. Toxins 2, 64–72.
Holmes, M.J., Lewis, R.J., 2023. Model of the origin of a ciguatoxic grouper (*Plectropomus leopardus*). Toxins 15.
Holmes, M.J., Lewis, R.J., Gillespie, N.C., 1990. Toxicity of Australian and French Polynesian strains of *Gambierdiscus toxicus* (Dinophyceae) grown in culture: characterization of a new type of maitotoxin. Toxicon 28, 1159–1172.
Holmes, M.J., Lewis, R.J., Poli, M.A., et al., 1991. Strain dependent production of Ciguatoxin precursors (Gambiertoxins) by *Gambierdiscus toxicus* (Dinophyceae) in culture. Toxicon 29, 761–775.
Hoppenrath, M., Murray, S.A., Chomérat, N., et al., 2023. Marine Benthic Dinoflagellates - their Relevance for Science and Society. Senckenberg, Germany.
Ikehara, T., Kuniyoshi, K., Oshiro, N., et al., 2017. Biooxidation of Ciguatoxins leads to species-specific toxin profiles. Toxins 9.
Inoue, M., Miyazaki, K., Uehara, H., et al., 2004. First and second generation total synthesis of Ciguatoxin CTX3C. Proceedings of the National Academy of Sciences of the USA. 101, 12013–12018.
Jang, S.H., Jeong, H.J., Yoo, Y.D., 2018. *Gambierdiscus jejuensis* sp. nov., an epiphytic dinoflagellate from the waters of Jeju island, Korea, effect of temperature on the growth, and its global distribution. Harmful Algae 80, 149–157.
Kibler, S.R., Tester, P.A., Kunkel, K.E., et al., 2015. Effects of ocean warming on growth and distribution of dinoflagellates associated with ciguatera fish poisoning in the Caribbean. Ecol. Model. 316, 194–210.
Kohli, G.S., Murray, S.A., Neilan, B.A., et al., 2014. High abundance of the potentially maitotoxic dinoflagellate *Gambierdiscus carpenteri* in temperate waters of New South Wales. Australia. Harmful Algae. 39, 134–145.
Kohli, G.S., John, U., Figueroa, R.I., et al., 2015. Polyketide synthesis genes associated with toxin production in two species of *Gambierdiscus* (Dinophyceae). BMC Genomics 16, 410.
Kohli, G.S., Haslauer, K., Sarowar, C., et al., 2017. Qualitative and quantitative assessment of the presence of Ciguatoxin, P-CTX-1B, in Spanish mackerel (*Scomberomorus commerson*) from waters in New South Wales (Australia). Toxicol. Rep. 4, 328–334.
Kretzschmar, A.L., Verma, A., Harwood, T., et al., 2017. Characterization of *Gambierdiscus lapillus* sp. nov. (Gonyaulacales, Dinophyceae): a new toxic dinoflagellate from the great barrier reef (Australia). J. Phycol. 53, 283–297.
Kretzschmar, A.L., Larsson, M.E., Hoppenrath, M., et al., 2019. Characterisation of two toxic *Gambierdiscus* spp (Gonyaulacales, Dinophyceae) from the Great Barrier Reef (Australia): *G. lewisii* sp. nov. and G. holmesii sp. nov. Protist 170, 125699.
Larsson, M.E., Laczka OF, Harwood, D.T., et al., 2018. Toxicology of *Gambierdiscus* spp. (Dinophyceae) from tropical and temperate australian waters. Mar. Drugs 16.
Ledreux, A., Brand, H., Chinain, M., Bottein, M.Y.D., Ramsdell, J.S., 2014. Dynamics of ciguatoxins from *Gambierdiscus polynesiensis* in the benthic herbivore *Mugil cephalus*: trophic transfer implications. Harmful Algae 39, 165–174.
Lehane, L., Lewis, R.J., 2000. Ciguatera: recent advances but the risk remains. Int. J. Food Microbiol. 61, 91–125.
Lewis, R.J., Endean, R., 1984. Ciguatoxin from the flesh and viscera of the barracuda. Sphyraena jello. Toxicon. 22, 805–810.
Lewis, R.J., Sellin, M., Poli, M.A., et al., 1991. Purification and characterization of Ciguatoxins from moray eel (*Lycodontis javanicus*, Muraenidae). Toxicon 29, 1115–1127.
Lewis, R.J., Inserra, M., Vetter, I., et al., 2016. Rapid extraction and identification of Maitotoxin and Ciguatoxin-like toxins from Caribbean and Pacific *Gambierdiscus* using a new functional bioassay. PLoS One 11, e0160006.
Litaker, R.W., Vandersea, M.W., Faust, M.A., et al., 2009. Taxonomy of *Gambierdiscus* including four new species, *Gambierdiscus caribaeus, Gambierdiscus carolinianus, Gambierdiscus carpenteri* and *Gambierdiscus ruetzleri* (Gonyaulacales, Dinophyceae). Phycologia 48, 344–390.
Litaker, R.W., Vandersea, M.W., Faust, M.A., et al., 2010. Global distribution of ciguatera causing dinoflagellates in the genus *Gambierdiscus*. Toxicon 56, 711–730.
Longo, S., Sibat, M., Viallon, J., et al., 2019a. Intraspecific variability in the toxin production and toxin profiles of in vitro cultures of *Gambierdiscus polynesiensis* (Dinophyceae) from French Polynesia. Toxins (Basel). 11, 735.
Longo, S., Sibat, M., Viallon, J., et al., 2019b. Intraspecific variability in the toxin production and toxin profiles of in vitro cultures of *Gambierdiscus polynesiensis* (Dinophyceae) from French Polynesia. Toxins 11.
Martin, M., 2011. Cutadapt removes adapter sequences from high-throughput sequencing reads. EMBnet Journal. 17, 10–12.
Munday, R., Murray, S., Rhodes, L.L., et al., 2017. Ciguatoxins and maitotoxins in extracts of sixteen *Gambierdiscus* isolates and one *Fukuyoa* isolate from the South Pacific and their toxicity to mice by intraperitoneal and oral administration. Mar. Drugs 15.
Murray, J.S., Boundy, M.J., Selwood, A.I., et al., 2018. Development of an LC-MS/MS method to simultaneously monitor maitotoxins and selected ciguatoxins in algal cultures and P-CTX-1B in fish. Harmful Algae 80.
Murray, S., Momigliano, P., Heimann, K., et al., 2014. Molecular phylogenetics and morphology of *Gambierdiscus yasumotoi* from tropical eastern Australia. Harmful Algae 39, 242–252.
Pisapia, F., Holland, W.C., Hardison, D.R., et al., 2017. Toxicity screening of 13 *Gambierdiscus* strains using neuro-2a and erythrocyte lysis bioassays. Harmful Algae 63, 173–183.
RCoreTeam R: A language and environment for statistical computing. R foundation for statistical computing, Vienna, Austria.
FAO, WHO. Report of the expert meeting on ciguatera poisoning. Rome, 19-23. Report, November 2018 2020.
Rhodes, L., Harwood, T., Smith, K., et al., 2014. Production of ciguatoxin and maitotoxin by strains of *Gambierdiscus australes, G. Pacificus* and *G. Polynesiensis* (Dinophyceae) isolated from Rarotonga, Cook Islands. Harmful Algae 39, 185–190.
Rhodes, L.L., Smith, K.F., Murray, S., et al., 2017. The epiphytic genus *Gambierdiscus* (dinophyceae) in the Kermadec islands and Zealandia regions of the southwestern Pacific and the associated risk of ciguatera fish poisoning. Mar. Drugs 15.
Rongo, T., Van Woesik, R., 2013. The effects of natural disturbances, reef state, and herbivorous fish densities on ciguatera poisoning in Rarotonga, southern Cook Islands. Toxicon 64, 87–95.
Simao, F.A., Waterhouse, R.M., Ioannidis, P., et al., 2015. Busco: assessing genome assembly and annotation completeness with single-copy orthologs. Bioinformatics 31, 3210–3212.
Skinner, M.P., Brewer, T.D., Johnstone, R., et al., 2011. Ciguatera fish poisoning in the Pacific Islands (1998 to 2008). PLoS Negl. Trop. Dis. 5, e1416.
Smith, K.F., Rhodes, L.L., Curley, B., et al., 2023. *Gambierdiscus* (Dinophyta: Alveolata) community structure shapes ciguatoxin risk in a tropical lagoon ecosystem. *http://dxdoiorg/102139/ssrn4620290*.
Sparrow, L., Momigliano, P., Russ, G.R., et al., 2017. Effects of temperature, salinity and composition of the dinoflagellate assemblage on the growth of *Gambierdiscus carpenteri* isolated from the great barrier reef. Harmful Algae 65, 52–60.
Tester, P.A., Feldman, R.L., Nau, A.W., et al., 2010. Ciguatera fish poisoning and sea surface temperatures in the caribbean sea and the west indies. Toxicon 56, 698–710.
Tester, P.A., Litaker, R.W., Berdalet, E., 2020. Climate change and harmful benthic microalgae. Harmful Algae 91, 101655.
Tonge, J.I., Battey, Y., Forbes, J.J., 1967. Ciguatera poisoning: a report of two outbreaks ana a probable fatal case in Queensland. Med. J. Aust. 1088–1090.
Verma, A., Hoppenrath, M., Dorantes-Aranda, J.J., et al., 2016. Molecular and phylogenetic characterization of *Ostreopsis* (Dinophyceae) and the description of a new species, *Ostreopsis rhodesae* sp. nov., from a subtropical Australian lagoon. Harmful Algae 60, 116–130.
Xu, Y., Richlen, M.L., Morton, S.L., Mak, Y.L., Chan, L.L., Tekiau, A., Anderson, D.M., 2014a. Distribution, abundance and diversity of *Gambierdiscus* spp. from a ciguatera-endemic area in marakei, republic of Kiribati. Harmful Algae 34, 56–68.
Xu, Y., Richlen, M.L., Morton, S.L., et al., 2014b. Distribution, abundance and diversity of *Gambierdiscus* spp. from a ciguatera-endemic area in Marakei, Republic of Kiribati. Harmful Algae 34, 56–68.
Yogi, K., Sakugawa, S., Oshiro, N., et al., 2014. Determination of toxins involved in ciguatera fish poisoning in the Pacific by LC-MS. J. AOAC Int. 97, 398–402.